Experiment and Analysis of Two-Photon Absorption Spectroscopy Using a White-Light Continuum Probe

Raluca A. Negres, Joel M. Hales, *Member, IEEE,* Andrey Kobyakov, *Member, IEEE,* David J. Hagan, and Eric W. Van Stryland

***Abstract*—We present an experimental technique along with the method of data analysis to give nondegenerate two-photon absorption (2PA) spectra. We use a femtosecond pump pulse and a white-light continuum (WLC) probe to rapidly generate the 2PA spectra of a variety of materials. In order to analyze data taken with this method, the spectral and temporal characteristics of the WLC must be known, along with the linear dispersion of the sample. This allows determination of the temporal walk-off of the pump and probe pulses as a function of frequency caused by group-velocity mismatch. Data correction can then be performed to obtain the nonlinear losses. We derive an analytical formula for the normalized nonlinear transmittance that is valid under quite general experimental parameters. We verify this on ZnS and use it for the determination of 2PA spectra of some organic compounds in solution. We also compare some of the data on organics with two-photon fluorescence data and find good agreement.**

***Index Terms*—Nonlinear transmission, nonlinear wave propagation, two-photon absorption coefficient, two-photon absorption cross section, white-light continuum.**

I. Introduction

THERE IS currently significant interest in finding materials with large nonlinearities for a variety of applications [1]. Of specific interest to this paper is two-photon absorption (2PA), with applications in the emerging technologies of, for example, optical power limiting [2], two-photon fluorescence imaging [3], two-photon photodynamic cancer therapy [4], and two-photon microfabrication [5].

With the relatively recent introduction of broadly tunable laser sources, and more recently the widely tunable optical parametric generation/amplification (OPA) sources, the field of nonlinear spectroscopy has opened to researchers in many new fields. However, in order to obtain reliable nonlinear absorption (NLA) measurements, the spectroscopist must pay careful attention to the source irradiance as a function of wavelength, λ_p. This added requirement over linear spectroscopy makes measurement much more difficult. The laser pulsewidth (and any possible temporal modulation), the laser beam's spatial distribution (and any possible changes with propagation through the sample), and the source energy must all be accurately monitored at each wavelength λ_p, in order to determine the irradiance $I(\lambda_p) = \mathrm{energy}(\lambda_p)/\mathrm{area}(\lambda_p)/\mathrm{time}(\lambda_p)$.

Despite these complications, there have been numerous successes in determining nonlinear spectra of many materials even with only a couple of wavelengths, e.g., 1.064 μm and 532 nm. For example, the Z-scan method has proven quite useful in separately measuring NLA and nonlinear refraction at single wavelengths for semiconductor and transparent dielectric materials [6]. However, for materials with more complicated electronic structure, such as complex organic compounds, multiple two-photon bands can occur. To date, no universal theory of structure property relations can predict these spectra, and the database of nonlinear spectra is sparse. To fill this void, a method is needed to rapidly monitor nonlinear spectra. The technique and analysis presented here is one such example.

The method of interest to us is femtosecond pump-probe spectroscopy where a broadband, weak, white-light continuum (WLC) [7]–[10] pulse is used to probe a medium that is subjected to an intense pump pulse. The result of this pump/probe technique is the nondegenerate NLA spectrum. This method could, in principle, be a single-shot technique, since the large spectral extent of the probe beam could allow for full characterization of the sample with a single laser pulse. However, in practice, the temporal delay between the pump and probe must be scanned since the WLC is strongly chirped so that temporal coincidence between the pump and probe (i.e., "zero delay") for one wavelength is different than for another wavelength. This chirp is due to the generation process itself, since the different colors of the continuum must propagate in the generation medium (e.g., sapphire, fused silica) where group velocity dispersion (GVD) temporally displaces each color [7]. This chirp results in a peak of the maximal 2PA signal that shifts in wavelength as the temporal delay between pump and WLC probe is varied. Corrections to the data for this effect on 2PA are straightforward. Alternative methods to obtain the spectral dependence of the nonlinearity involve more time-consuming processes of tuning and calibration of the probe and/or pump pulses at various different wavelengths in Z-scan and/or degenerate pump-probe experiments, which give the degenerate nonlinearity. Furthermore, the nondegenerate NLA spectrum obtained from our experiment, under certain conditions [11], can be used to infer the spectral dependence of the nonlinear refraction through the Kramers–Krönig relationships [12].

Manuscript received March 18, 2002; revised May 31, 2002. This work was supported by the National Science Foundation under Grant 9970078, by the Office of Naval Research under Grant N00014-97-1-0936, by the Naval Air Warfare Center Joint Service Agile Program under Contract N00421-98-C-1327, and by the Air Force Office of Scientific Research under Grant F49620-93-C-0063.

R. A. Negres, J. M. Hales, D. J. Hagan, and E. W. Van Stryland are with the School of Optics/CREOL, University of Central Florida, Orlando, FL 32816-2700 USA.

A. Kobyakov is with the Photonics Research and Test Center, Corning Incorporated, Somerset, NJ 08873 USA.

Publisher Item Identifier 10.1109/JQE.2002.802448.

The potential disadvantage of the need to scan the temporal delay between pump and WLC probe can be used as an advantage in distinguishing the physical mechanisms behind the nonlinearity. For example, "instantaneous" nonlinearities such as 2PA occur only for zero delay where the pump and probe pulses are temporally overlapped, while longer-lived nonlinearities such as excited-state or carrier nonlinearities will remain for some time after excitation. However, the experimentally determined raw data must be corrected for both the chirp of the continuum described above and the temporal walk-off due to group-velocity mismatch, which varies with probe wavelength. We will describe this latter correction in detail in this paper. Fortunately, we have determined an analytical relationship that allows for a simple correction given knowledge of the linear dispersion of the sample and a full characterization of the chirp of the WLC, i.e., the relation between wavelength and time. The WLC characterization can be performed by a cross-correlation technique where some instantaneous nonlinear process, such as SHG or the optical Kerr effect (which is preferable since no phase-matching is required), is used to obtain the cross-correlation signal [8], [13], [14].

Given the above WLC characterization, the temporal correction for the chirp is not difficult to implement; however, the nondegenerate character of the experiment means that pump and probe pulses travel through the sample at different group velocities and can physically walk-off from one another in time within the sample. This is important in our setup where the pump wavelength is set at a wavelength below half the bandgap of the material under study in order to avoid any degenerate 2PA by the pump itself. This walk-off causes the effective interaction length to be significantly reduced compared to the degenerate case (where the pump and probe pulses at the same frequency travel with equal group velocities within the sample), and will reduce the magnitude of the nonlinear signal. This is a purely linear phenomenon and can be accounted for in the data analysis. We note here the work undertaken by Ziólek *et al.* [15] that illustrates how the real temporal response function of a pump-probe apparatus can be determined if the linear properties of the sample (dispersion of refractive index) are known. In this paper, we present a general model including linear and nonlinear effects for the pump-probe interaction in Kerr media for a 2PA process, in particular. Furthermore, the single dynamical equation we find to model this interaction allows us to determine the impact of each individual parameter on the nonlinear signal.

The effects of temporal walk-off and the initial time delay between pulses on the magnitude of the nonlinear signal are analyzed in Section II. We find that we can treat the continuum as made up of a superposition of nearly bandwidth-limited pulses of different central wavelengths, which we will henceforth refer to as *bandwidth-limited probe* pulses to distinguish them from the entire WLC probe. This considerably simplifies the analysis and is valid, provided there is minimal cross-phase modulation between adjacent *bandwidth-limited probe* pulses in the full WLC. This will be illustrated in Section IV. An analytic solution for the normalized fluence transmittance can be found in the limit where the pulsewidth for any given wavelength of the continuum does not change within the sample (this is the limit of vanishing GVD). This approximation holds true for thin samples not exceeding a few millimeters in thickness and for pulsewidths in the 100-fs range. However, the group velocity mismatch (GVM) must be known to determine the temporal walk-off between pump and *bandwidth-limited probe* at different wavelengths. The formula derived is used in fitting the 2PA experimental data from transient absorption spectroscopy on a semiconductor sample, ZnS, and on solutions of organic dyes. The agreement with previous results and with theory on ZnS confirms the validity of the solution. A preliminary report of this model and results were recently presented in a more concise form in [16].

This paper is organized as follows. Section II outlines the theoretical analysis for the nondegenerate pump-probe interaction in a nonlinear medium, taking into account linear propagation effects. In Section III, we present the experimental set-up and the methods used for acquiring the transient absorption data on a semiconductor sample. Section IV shows the chirp-corrected data and illustrates the effect of correcting the data for walk-off artifacts via the equations presented in Section II. We compare the results of the nondegenerate 2PA spectrum with the degenerate two-photon fluorescence spectrum obtained on organic molecules having a large linear dipole moment in Section V. Finally, Section VI concludes the paper with future plans.

II. Pump–Probe Interaction in Kerr Media

Using Maxwell's equations to derive the nonlinear wave equation, assuming a weak *bandwidth-limited probe* and an excitation wavelength chosen such that it has no linear or degenerate 2PA, we find the spatial-temporal evolution of the *bandwidth-limited probe* wave field E (defined as $E(z,t) = 1/2E(z,t)e^{i(kz-\omega t)} + \text{c.c.}$) centered at wavelength λ (angular frequency ω), is given by the equation [17], [18]

$$i\left(\frac{\partial E}{\partial z}+\frac{\alpha}{2}E+\frac{1}{\nu}\frac{\partial E}{\partial t}\right)-\frac{1}{2}D\frac{\partial^2 E}{\partial t^2}+2\gamma|E_p|^2E=0 \tag{1}$$

where subscript p refers to the pump wave, while the symbols without a subscript stand for the *bandwidth-limited probe* wave. Again, we are using a nearly bandwidth-limited pulse as the *bandwidth-limited probe* as opposed to the entire WLC probe. Here, α and n are the linear absorption coefficient and refractive index for the *bandwidth-limited probe*, ν is the group velocity given by

$$\frac{1}{\nu}=\frac{dk}{d\omega}=\frac{1}{c}\left(n-\lambda\frac{dn}{d\lambda}\right) \tag{2}$$

and D accounts for the group velocity dispersion

$$D=\frac{d^2k}{d\omega^2}=\frac{\lambda^3}{2\pi c^2}\frac{d^2n}{d\lambda^2}. \tag{3}$$

The nonlinear interaction between the two waves is represented by the complex cross-phase modulation term (last term) with the pump field assumed constant along the propagation coordinate z and

$$\gamma=\frac{3\pi}{4\lambda n}\chi^{(3)}(-\omega;-\omega_p,\omega_p,\omega). \tag{4}$$

This approximation, known as the undeleted pump approximation, is valid due to our choice of a pump photon energy which has no 2PA and negligible linear loss. We introduce dimensionless variables. For instance, the normalized time $T = t/w_p$ is scaled with the temporal width of the pump pulse w_p (HW1/eM of irradiance), and the normalized propagation distance $Z = z/L$ is scaled with the total sample length L, i.e., $0 \le Z \le 1$. To further simplify our analysis, we choose the coordinate system (Z, τ) that moves with the group velocity of the pump wave ν_p, i.e., $\tau = T - z/(\nu_p w_p)$. As a result, (1) takes the form

$$i\left(\frac{\partial a}{\partial Z} + \sigma a + \rho\frac{\partial a}{\partial \tau}\right) - \mu\frac{\partial^2 a}{\partial \tau^2} + \chi|a_p|^2 a = 0 \qquad (5)$$

where $a(Z,\tau) \equiv E(Z,\tau)/E_p(0,\tau), \sigma = \alpha L/2$ is the normalized linear absorption, and the GVM parameter is given by

$$\rho = \frac{L}{w_p c}\left\{n - \lambda\left.\frac{dn}{d\lambda}\right|_{\lambda} - \left[n_p - \lambda_p\left.\frac{dn}{d\lambda}\right|_{\lambda_p}\right]\right\} = \frac{L}{w_p c}\Delta n_g \qquad (6)$$

where Δn_g is just the difference in group indices. The GVD parameter is defined as

$$\mu = \frac{\lambda^3 L}{4\pi c^2 w_p^2}\left.\frac{d^2 n}{d\lambda^2}\right|_{\lambda} \qquad (7)$$

which is simply $L/(2w_p^2)D$. The corresponding dimensionless nonlinear coefficient can be written as

$$\chi \equiv \eta + i\Gamma = 4\pi\frac{L}{\lambda}\frac{n}{n_p}I_p^0 n_2^I + iL\frac{n}{n_p}I_p^0\beta \qquad (8)$$

where I_p^0 is the peak irradiance (in W/m^2) of the pump wave, n_2^I is the nondegenerate nonlinear refraction coefficient defined by $n = n_0 + n_2^I I$ (in m^2/W), and β is the nondegenerate 2PA coefficient, defined by $dI/dz = -2\beta I_p I$ (in m/W). In the framework of the undepleted pump approximation, we have $a_p(Z,\tau) \equiv a_p(\tau)$. If we assume Gaussian temporal profiles for the pump

$$a_p(\tau) = \exp\left(-\frac{\tau^2}{2}\right) \qquad (9)$$

and for the *bandwidth-limited probe* waves, the boundary condition for (5) can be written as

$$a(0,\tau) = A\exp\left(-\frac{1}{2}\frac{[\tau+\tau_d]^2}{W^2}\right) \qquad (10)$$

where $A = \sqrt{I^0/I_p^0}$ and $W = w/w_p$ are the ratios of the *bandwidth-limited probe* and pump amplitudes and widths, respectively, and τ_d is the initial delay time between the pump and the *bandwidth-limited probe* (the term is dimensionless since it is the ratio of the initial time delay to the pump pulsewidth).

We now have a working form for the propagation of the *bandwidth-limited probe* field in the nonlinear medium and are able to look at temporal walk-off effects on the beam. Equation (5) with the boundary condition (10) can be solved numerically using the split-step Fourier transform method (see [18]). Although the split-step Fourier transform method is relatively fast, numerical studies of the impact of any parameter such as the pump-*bandwidth-limited probe* delay time, the ratio of pulsewidths, walk-off, or pump irradiance on nonlinear absorption becomes extremely time consuming. For this kind of study, an analytical solution to (5) would considerably expedite the quantitative analysis of the problem. Furthermore, this type of solution is essential when attempting to fit experimental data to the theoretical model. To find a general analytical solution of (5) with boundary condition (10) is a difficult task, but the problem simplifies considerably in the limit of a vanishing GVD parameter μ, i.e., where the fourth term in (5) can be neglected. This assumption is equivalent to assuming that the *bandwidth-limited probe* pulse does not broaden in time in transmission through the sample. We found numerically a quantitative upper limit for this "dispersionless'" approximation, and it is stated later in this section. Fortunately, for our purposes, this is exactly the experimental case when the pump-*bandwidth-limited probe* measurements are typically performed in thin samples where the pulsewidths involved are $\sim$100 fs. Once again, we note that the continuum is assumed to be composed of independent, nearly bandwidth-limited pulses, since the continuum itself considerably broadens in time. This is explained in more detail in the experimental section.

We take as an example ZnS, which has an extremely large temporal walk-off. A close look at the dispersion of the refractive index of ZnS over the probe spectrum of 0.4 μm $\le\lambda \le$ 0.75 μm and $\lambda_p = 0.75$ μm, shows that the temporal walk-off parameter varies over a wide range ($0 \le \rho \le 40$), while the dispersion parameter remains small $\mu <$0.31. Thus, for the approximate analysis, we will neglect dispersion (GVD term) and rewrite (5) as

$$\frac{\partial a}{\partial Z} + \rho\frac{\partial a}{\partial \tau} = f(\tau)a, \quad \text{with } f(\tau) = -\sigma + i\chi|a_p(\tau)|^2. \qquad (11)$$

Equation (11) can be easily solved by the substitution $u = \ln a$ with a subsequent transformation of variables $\xi = Z - (\tau/\rho), \zeta = \tau$. Then, (11) becomes $(\partial u/\partial\zeta) = (f(\zeta)/\rho)$ and its solution is $u(\xi,\zeta) = u_0(\xi) + (1/\rho)\int f(\zeta)\,d\zeta$, where $u_0(\xi)$ is determined by the incident pulses given by (9) and (10). Returning to the initial variables, we obtain a general solution to (11) as follows:

$$a(Z,\tau) = h\left(Z - \frac{\tau}{\rho}\right)\exp\left(-\frac{\sigma}{\rho}\tau + i\frac{\chi}{\rho}\int |a_p(\tau)|^2\,d\tau\right) \qquad (12)$$

where h is again a function determined by the boundary conditions. This solution is valid for any pump and *bandwidth-limited probe* temporal profile. For a Gaussian pump and *bandwidth-limited probe* pulse, the solution takes the form

$$a(Z,\tau) = A\exp\left(-\frac{1}{2}\left(\frac{\tau+\tau_d-\rho Z}{W}\right)^2 - \sigma Z + i\frac{\chi\sqrt{\pi}}{2\rho}[\operatorname{erf}(\tau) - \operatorname{erf}(\tau-\rho Z)]\right) \qquad (13)$$

where $\operatorname{erf} x = (2/\sqrt{\pi})\int_0^x \exp(-y^2)\,dy$. In the limit of vanishing walk-off $\rho \to 0, \lim_{x\to 0}(\operatorname{erf}\tau - \operatorname{erf}(\tau - x))/(x) = (2\exp(-\tau^2))/(\sqrt{\pi})$.

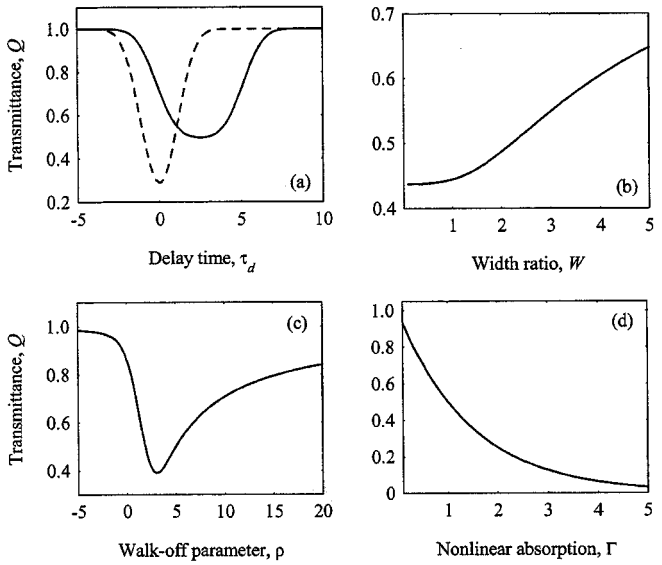

Fig. 1. Probe pulse propagation in ZnS. Probe pulse profile ($\lambda = 0.6\ \mu$m) at (a) $Z = 0.5$ and (b) $Z = 1$. Solid curves: analytical formula (13). Triangles: results of numerical integration of (5). Initial probe profile (10) is shown for reference by dashed lines.

As an example, prior to the analysis of the 2PA chirp-corrected data (in Section IV), we look at the effects of linear propagation on the nonlinear transmittance in a 0.84-mm long ZnS sample. Linear and nonlinear parameters for ZnS are taken from [19]. We calculate the material parameters at three different *bandwidth-limited probe* wavelengths (physical parameters, prior to normalization, are given in parentheses):

1) $\lambda = 0.5\ \mu$m, $\sigma = 0.1$ ($\alpha \cong 1.2\,\text{cm}^{-1}$), $\rho = 13.5$ ($\Delta n_g = 0.35$), $\mu = 0.1$ ($D = 1200\ \text{fs}^2/\text{mm}$);
2) $\lambda = 0.6\ \mu$m, $\sigma = 0.06$ ($\alpha \cong 0.7\,\text{cm}^{-1}$), $\rho = 5.1$ ($\Delta n_g = 0.13$), $\mu = 0.07$ ($D = 860\ \text{fs}^2/\text{mm}$);
3) $\lambda = 0.7\ \mu$m, $\sigma = 0.05$ ($\alpha \cong 0.6\,\text{cm}^{-1}$), $\rho = 1.2$ ($\Delta n_g = 0.03$), $\mu = 0.05$ ($D = 600\ \text{fs}^2/\text{mm}$).

Again, Δn_g is the difference in group index for pump and *bandwidth-limited probe as previously defined*. The other parameters of the simulations from (5) and (10) are as follows: $A = 0.1, W = 0.85$ and $\tau_d = 2$. The pump pulse is assumed to be Gaussian with a peak irradiance $I_0^p = 2.5\,\text{GW/cm}^2$, $w_p = 72$ fs, and $\lambda_p = 0.75\ \mu$m ($hc/\lambda_p = 1.65$ eV). The choice of pump wavelength satisfies the first condition stated at the beginning of this section, i.e., no linear or degenerate 2PA of the pump. For the purpose of illustrating the degree to which the linear propagation parameters affect the nonlinear transmittance, we use the same values of the nonlinear coefficients for each *bandwidth-limited probe* wavelength, even though these are known to vary strongly with wavelength [20]. We use $\chi = 4.0 + i1.09$ ($n_2 = 7 \cdot 10^{-5}$ cm^2/GW, $\beta = 5$ cm/GW), which are values calculated from the theoretical model given in [21] for a pump wavelength of 750 nm and a *bandwidth-limited probe* wavelength of 480 nm. In order to check the validity of this dispersionless approximation, we compare the results of numerical integration of (5) with predictions of the analytical formula (13). Figs. 1(a) and (b) show that the analytical results are in excellent agreement with the numerics in these approximations.

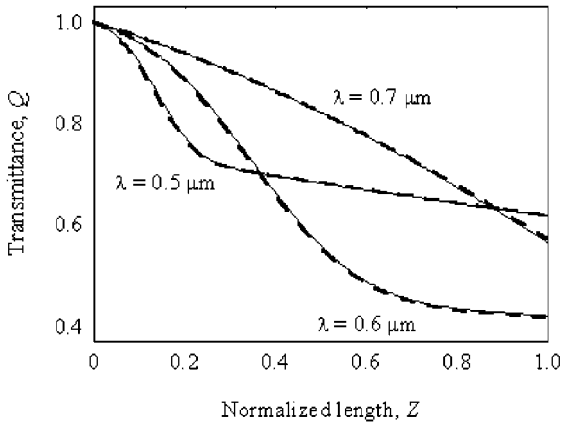

Fig. 2. Transmittance of the probe fluence at different wavelengths as a function of normalized length for ZnS. Solid curves: analytical formula (14). Dashed curves: numerical integration of (5). Pump is at $\lambda_p = 0.75\ \mu$m, with an irradiance of $I_0^P = 2.5$ GW/cm^2 and pulsewidth of $w_p = 72$ fs. The values used for β are held constant for each probe wavelength. All other constants are the same as those used for Fig. 1.

From this analytical formula, it is straightforward to obtain an expression for the transmittance of the fluence $F(Z) = \int_{-\infty}^{\infty} |a(Z,\tau)|^2\, d\tau$, defined as the ratio of the output and input fluence, or the nonlinear transmittance $Q = F(1)/F(0) \equiv T_{\text{NL}}$ ($Z = 1$ or $z = L$ corresponds to the output of the sample). Using (13) and (10), we obtain the final analytical result for the fluence transmittance, assuming Gaussian temporal pulse shapes, as follows:

$$Q(\sigma,\tau_d,W,\rho,\Gamma) = \frac{\exp(-2\sigma)}{W\sqrt{\pi}} \int_{-\infty}^{\infty} \exp\left\{ -\left(\frac{\tau+\tau_d-\rho}{W}\right)^2 - \frac{\Gamma\sqrt{\pi}}{\rho}[\text{erf}(\tau) - \text{erf}(\tau-\rho)] \right\} d\tau. \quad (14)$$

This formula, for the case of vanishing temporal walk-off, $\rho \to 0$, becomes the equation for degenerate 2PA

$$Q(\sigma,\tau_d,W,\Gamma) = \frac{\exp(-2\sigma)}{W\sqrt{\pi}} \times \int_{-\infty}^{\infty} \exp\left\{ -\left(\frac{\tau+\tau_d}{W}\right)^2 - 2\Gamma\exp(-\tau^2) \right\} d\tau. \quad (15)$$

In the absence of the nonlinearity, i.e., with the pump pulse blocked, the linear transmittance of the *bandwidth-limited probe* fluence can be easily calculated from (14) by setting $\Gamma = 0$, which gives $T_L = \exp(-2\sigma)$.

Three different scenarios of the transmittance evolution calculated from (14) and from the numerical solution of (5) are shown in Fig. 2. All the simulations use the same numerical parameters as previously listed in this section for ZnS. Again, the comparison shows good accuracy for the analytical results. We note that it is important that we assume the *bandwidth-limited probe* pulse to be a nearly bandwidth-limited portion of the WLC. This allows us to assume that the *bandwidth-limited probe* chirp does not lead to significant pulse broadening as the probe propagates through the thickness of the sample. However, in addition, we assume that the nonlinearly induced

phase modulation does not lead to a change of the pulsewidth within the sample. This is the reason that only the imaginary part of the nonlinear susceptibility, Γ, enters (14). Both of these assumptions are important for analysis because they exclude effects of pulse chirping (linear or nonlinear) in determining 2PA. We have found numerically that a quantitative estimate for the applicability of the linear *dispersionless* approximation is $\mu < \mu_{\rm cr} \approx 0.45$. This works in many materials if the sample length does not exceed several millimeters, and the pulsewidth is in the 100-fs range. To neglect the nonlinear pulse-chirping effects, the peak nonlinearly induced phase shift cannot be too large. However, we have found that this requirement is not very restrictive numerically, and even with a 2π phase shift the distortion is small. The inclusion of nonlinear phase effects inevitably reduces the critical value for μ, as listed above; however, this only becomes substantial for the pump pulse. We note that even in the extreme case of ZnS illustrated here, the dispersionless approximation remains valid for both linear and nonlinear propagation effects.

However, neglecting the real part η of the nonlinear susceptibility also implies that cross phase modulation (xpm) effects between the pump and *bandwidth-limited probe* are negligible. This requires qualification, considering the many studies which have concentrated on the effects of xpm on transient absorption spectroscopy [22]–[24]. For instance, Ekvall *et al.* [24] provide an extensive study of the effects on pump-probe measurements in a nonabsorbing medium with a Kerr nonlinearity. They explain why, in certain cases, unwanted xpm effects obscure transient absorption signals. However, although we have seen evidence of these artifacts their magnitude is quite small, providing a change in Q [(14)] of less than 1%, whereas most of our experimental two-photon absorption signals are greater than 10%. Therefore, we subsequently ignore these artifacts. We will qualify this statement in Section VI.

Since both the linear absorption σ and dispersion μ coefficients are small, the essential parameter that governs the *bandwidth-limited probe* evolution is the temporal walk-off ρ. This parameter is responsible for the relative speed of the *bandwidth-limited probe* and pump pulse envelopes, and consequently for the temporal overlap between them which, in turn, determines the strength of the nonlinear absorption. The closer the *bandwidth-limited probe* and pump wavelengths are to each other in wavelength, the slower the *bandwidth-limited probe* pulse moves with respect to the pump due to normal dispersion. At the exit face of the sample, the beams are separated in time from each other according to their initial delay τ_d and ρ. However, this group velocity mismatch affects the absorption of the *bandwidth-limited probe* in a nonmonotonic way. Pulses with relative velocities that are too fast are weakly absorbed, since they only overlap over a small depth within the sample. On the other hand, for a particular initial time delay τ_d, pulses that move too slowly may never overlap. The *bandwidth-limited probe* pulse corresponding to an intermediate walk-off is most strongly absorbed for a particular τ_d. Of course, for $\tau_d = 0$ (i.e., the pump and *bandwidth-limited probe* pulses perfectly overlapped at the front of the sample), the largest nonlinear loss occurs at degeneracy. We will discuss this dependence in more detail below.

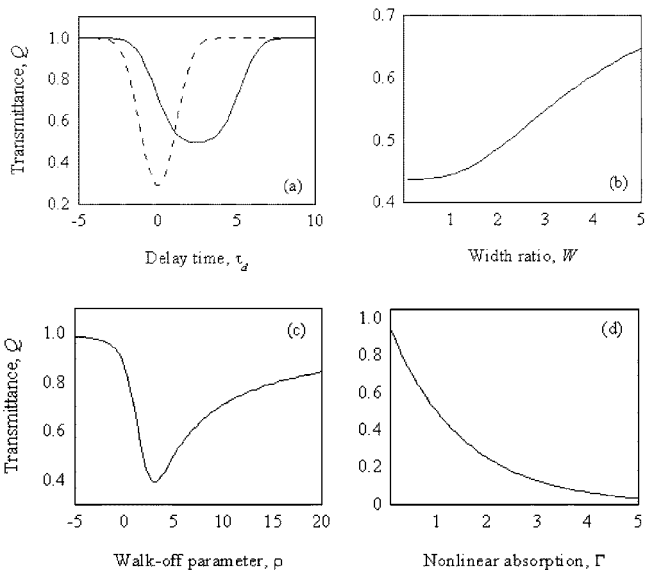

Fig. 3. Transmittance Q calculated from (14) as a function of: (a) delay time τ_d with $W = 1, \rho = 5, \Gamma = 1$ (solid line); (b) probe-pump width ratio $W = w/w_p$ with $\tau_d = 2, \rho = 5, \Gamma = 1$; (c) walk-off parameter ρ with $\tau_d = 2, W = 1, \Gamma = 1$; and (d) nonlinear absorption Γ with $\tau_d = 2, W = 1, \rho = 5$. The case of vanishing temporal walk-off [(15)] is shown in (a) by the dashed line, with $W = 1$ and $\Gamma = 1$. For all calculations, linear absorption is assumed to be negligible, $\sigma = 0$.

In Fig. 3, we show how we can use the analytical form (14) to quantitatively study the effect of the delay time, the *bandwidth-limited probe*-pump width ratio, the walk-off parameter, and the strength of the nonlinear absorption on the output transmittance. A plot similar to the one shown in Fig. 3(a) [solid line given by (14)] will be used to fit experimental 2PA cross-correlation signals (nonlinear signal versus time delay for a fixed *bandwidth-limited probe* wavelength). We discuss this procedure in detail in Section IV. If (15)—which ignores the temporal walk-off— is to be used instead, the dashed curve in Fig. 3(a) is obtained for the same parameters W and Γ. Here, not only is the magnitude of the nonlinear signal overestimated (for the same nonlinearity), but the temporal shape is greatly distorted.

The conclusion for this section on theoretical analysis is that the 2PA coefficient of the material can be accurately measured as a function of the wavelength if: 1) the linear properties of the material (dispersion relation and linear absorption) are known or determined from *a priori* WLC characterization experiments and 2) the shape of the WLC probe pulse is accurately characterized (i.e., *bandwidth-limited probe* pulsewidth at each wavelength together with the delay time with respect to the pump pulse). Then, (14) can be used to fit experimental data to determine the 2PA coefficient, provided that the sample is thin enough for the dispersionless limit to hold true.

III. Experimental Setup

The development of an analytic solution to the *bandwidth-limited probe* beam propagation in the nonlinear medium allows us to confirm its validity with quantitative data. The model described above has been applied in the transient absorption measurements in which the WLC (as a superposition of nearly bandwidth-limited pulses) serves as the *bandwidth-limited probe*,

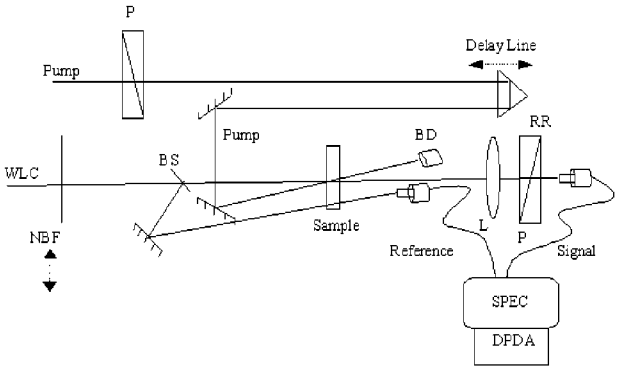

Fig. 4. Experimental setup for time-resolved spectroscopy. The spectra of white light continuum, signal, and reference are recorded versus the time delay between pump and probe beams. BS: Beamsplitter. L: Lens. P: Calcite GLAN polarizer. NBF: Narrow-bandwidth filter (used in narrowband measurements, only). RR: Retroreflector. BD: Beam dump. SPEC: Dual-fiber input spectrometer. DPDA: Dual photodiode array.

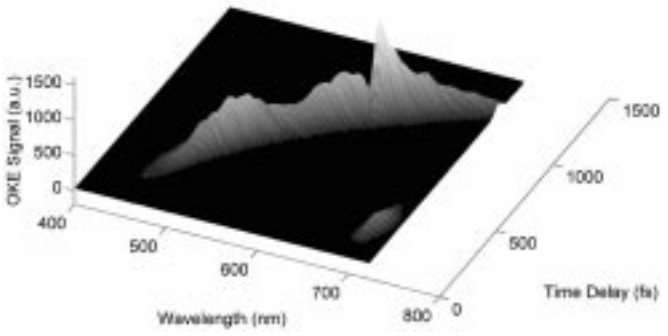

Fig. 5. OKE in Hexane ($L = 1$ mm, $\lambda_p = 0.75$ μm). The path of the signal follows the temporal dispersion of frequencies in the continuum probe pulse.

while a pulse at a wavelength of negligible linear absorption as well as 2PA is used as the pump.

The femtosecond laser used is a Ti:sapphire-based CPA-2001 system (CLARK-MXR) which provides laser pulses at 775 nm of 120-fs duration, with an energy of 0.94 mJ/pulse at a 1-kHz repetition rate. The laser pumps two optical parametric amplifier systems (TOPAS, Light Conversion), tunable over a broad range in the near-infrared and/or visible. 1–2 μJ of 1400 nm light is focused tightly into a 1.5-mm-thick piece of fused silica for generation of the probe WLC pulse. The experimental set-up is shown for reference in Fig. 4 and a detailed description can be found in [25]. We note that the pump and *bandwidth-limited probe* pulses are set at parallel polarizations.

We performed experiments in two arrangements. First, the transmitted spectrum of the WLC (or the probe pulse, which spatially overlaps the pump pulse within the sample) is registered as a function of time delay between pump and *bandwidth-limited probe* pulses. A second probe pulse (reference pulse) is sent through an unexcited portion of the sample to monitor the linear transmittance. A dual-fiber input spectrometer is used for this purpose (SpectraPro 150, Acton Research), which itself is coupled to a dual diode array (Princeton Instruments Silicon DPDA 2048 for visible 300–1100 nm or Sensors Unlimited InGaAs DPDA 512 for infrared 800–1700 nm). In what follows, we refer to this setup as the spectral measurement. In the second arrangement, narrow-band filters ($\sim$10 nm), centered at various wavelengths throughout the spectral range of interest, are inserted in the continuum path and the probe transmission is recorded versus time delay using photodiodes. This method gives a better signal-to-noise ratio than the spectral method $(\mathrm{S/N} \sim 200)$, but takes much more time to acquire than the spectral data. This arrangement provides the narrowband measurements discussed below.

As previously mentioned, in order to correct the NLA spectral data, the WLC must be fully characterized. This can be accomplished using optical Kerr effect (OKE) measurements performed in, for example, fused silica (details of these preliminary experiments can be found in [13], [14], [25]). The OKE technique provides a distinct advantage over other methods, such as frequency-resolved optical gating (FROG) [26], since only minimal changes in the transient absorption set-up are required (i.e., rotation of the pump polarizer and probe analyzer). This experiment maps the frequency content of the continuum in the time domain and illustrated in Fig. 5. For WLC generation with 1400 nm focused into the 1.5-mm piece of fused silica, the time arrival of various wavelengths in the continuum has been found to obey the following equation:

$$\tau_{\mathrm{oke}} = 7.42 \times 10^4 \cdot \left(\frac{1}{\lambda}\right)^4 - 3.92 \times 10^5 \cdot \left(\frac{1}{\lambda}\right)^2 + 0.7 \tag{16}$$

where λ is in nanometers and τ_{oke} in picoseconds. We performed the OKE measurements using a sample of hexane with a pathlength of 1 mm. The pump wavelength is, just as in the transient absorption experiments, λ_p =750 nm. From this measurement, we can estimate the rate of chirp of the continuum to be about 3.5 fs/nm. From OKE cross-correlation traces (signal versus time at any fixed λ), the pulse duration within each spectral interval ($\sim$5 nm) of the continuum pulse can also be inferred given the duration of the pump pulse at 750 nm. The deconvolution assumes Gaussian-shaped pulses for both pump and *bandwidth-limited probe*, and thus for the cross-correlation signal as well. The continuum is described as made up of a group of nearly bandwidth-limited pulses centered at various wavelengths whose duration can be calculated from a simple relation $\tau_{\mathrm{cc}}^2 = \tau_{\mathrm{wlc}}^2 + \tau_p^2/2$, where the subscripts cc and wlc refer to the cross-correlation signal and narrow bandwidth continuum pulse, respectively. The probe pulse duration is needed for the walk-off analysis given in Section II. The pulsewidth turns out to be constant over the entire visible range used in these experiments and is 100 fs $\pm$ 10 fs (FWHM), which is equal to the duration of the pump at 1400 nm used for continuum generation. One more crucial advantage of the OKE method is that, similar to white-light interferometry, one can measure the GVD of an unknown sample inserted in the WLC path. From OKE measurements, with and without the sample in the probe path, the difference in arrival time for a fixed-frequency component of the continuum gives the group index of the material. This is needed for materials whose dispersion is not yet in any database. Results of GVD measurements in ZnS and organic samples are presented in Section IV.

The time delay of the *bandwidth-limited probe* pulse with respect to the pump is varied in small increments ($\sim$20 fs) to accurately sample the fast nonlinear process of 2PA. The recorded

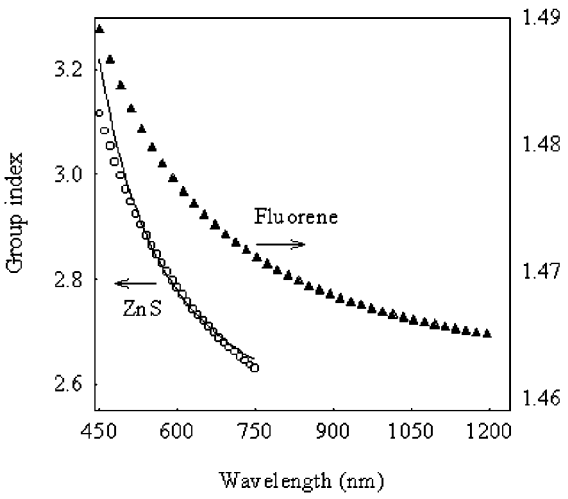

Fig. 6. Group index measurements using OKE in Hexane for ZnS, $L = 0.84$ mm (open circles) and fluorene derivative, $L = 1$ mm (open triangles). Sellmeier's equation for ZnS (18) is shown for reference (solid line).

spectra versus time delay along with the continuum chirp information are then used in reconstruction of the nonlinear absorption spectrum. At this point, the resultant spectrum must be corrected for the linear effects of pump-*bandwidth-limited probe* propagation within the sample (e.g., temporal walk-off). The reconstructed nonlinear absorption spectrum after chirp correction is the subject of the analysis presented in Section II.

We use (14) to fit the cross-correlation signals from the transient absorption measurements (i.e., normalized *bandwidth-limited probe* transmittance versus time delay) at various *bandwidth-limited probe* wavelengths (every 10 nm) within the WLC spectrum where the 2PA signal is present. This yields the corrected values of the nondegenerate 2PA coefficients at each *bandwidth-limited probe* wavelength.

IV. Results

Prior to transient absorption experiments, we have performed the OKE experiments described in the previous section to obtain the GVD in our samples. Our ZnS sample, provided by Eagle-Picher, has a polytype structure in which alternating layers of random hexagonal and cubic phases make the sample appear isotropic. With the ZnS sample inserted in the WLC path, we obtain a second OKE trace, similar to the one in Fig. 5. The temporal chirp of the WLC probe in this new configuration is given by

$$\tau'_{\text{oke}} = 3.55 \times 10^5 \cdot \left(\frac{1}{\lambda}\right)^4 - 8.88 \times 10^5 \cdot \left(\frac{1}{\lambda}\right)^2 + 3.2. \tag{17}$$

The difference in the arrival times at each wavelength, from (16) and (17), is simply related to the group index through $n_g = c \cdot (\tau_{\text{oke}} - \tau'_{\text{oke}})/(L)$. The results are presented in Fig. 6. For ZnS, we also compare the measured group index (open circles) to the one calculated from Sellmeier's equation, which is found in [19] and is valid in the 0.36–1.4-μm region

$$n(\lambda)^2 = 4.4175 + 1.7396\frac{\lambda^2}{\lambda^2 - 0.2677^2}, \quad \lambda \text{ in } \mu\text{m}. \tag{18}$$

The OKE experiments are easily performed in our transient absorption setup with minimal changes and offer reasonable values for the group index of organic dyes in solution, where Sellmeier's equation is not available. Additionally, the theoretical fittings for the temporal dependence of the 2PA signals given below verify the utility of this method. Once again, we used the OKE method to determine the temporal walk-off (ρ) as a function of wavelength, such that when fitting our 2PA cross-correlation signals, we only require one fitting parameter, the nonlinearity (Γ) [see (14)]. However, we make note here that ρ can be used as a second fitting parameter in the analysis of 2PA, along with the nonlinearity Γ. When both ρ and Γ are used as simultaneous fitting parameters, a comparison of the values of walkoff obtained from the fitting with those obtained from the OKE analysis reveals relative errors between the methods of less than 20%. This implies that an additional method (outside the transient absorption experiment itself) may not be necessary to determine the temporal walk-off as a function of wavelength. However, for small cross-correlation signals, OKE data provide a very good starting point for the fitting procedure.

We can now start the detailed analysis (as described in Section II) of the nondegenerate 2PA raw data obtained for the semiconductor sample, ZnS. This material has been well characterized in the past and data on the 2PA coefficients can be found in the literature [27]. A theoretical model has also been developed and its predictions agree well with past experimental data, for both semiconductors and dielectrics [21], [27], [28].

We can now calculate the walk-off ρ and dispersion parameter μ that enter in the calculations of 2PA for this sample [defined in (6) and (7)]. We use a pump pulse at 750 nm and pulsewidth $\tau_p = 120$ fs (FWHM). The length of the ZnS sample is $L = 0.84$ mm. The dispersion parameter is below the critical value of $\sim$0.45 found in Section II and will be ignored from now on ($\mu < 0.31$ over the visible range). The linear absorption of the sample is also small ($\sigma < 0.12$). With a pump wavelength of 750 nm and a bandgap of E_g =3.54 eV, the visible photons in the continuum probe that are absorbed simultaneously with the pump photons should have $\lambda \leq 660$ nm. We can foresee that the large values for the walk-off parameter in the short wavelength range will make a substantial difference when the chirp-corrected 2PA data is analyzed taking this parameter into account [(14)] as opposed to when it is not [(15)].

The experiments performed on this sample include transient absorption measurements using the WLC probe in both scenarios described above, spectral and narrowband measurements. Typical raw WLC spectra recorded at consecutive time delays are displayed in Fig. 7 in a similar fashion to the spectrogram of a femtosecond pulse, which is obtained in a FROG setup [26]. The contour of the nonlinear signal versus *bandwidth-limited probe* wavelength resembles the chirp of the continuum beam, shorter wavelengths arriving at the sample much later than the longer wavelengths according to the chirp rate. The envelope of consecutive spectra (maximum change in transmission versus *bandwidth-limited probe* wavelength) will be the chirp-corrected nonlinear absorption spectrum of the sample. As mentioned above, our experiment monitors not only the nonlinear transmittance, but also the linear transmittance as well, using a reference beam (see Fig. 4). Therefore, the z axis in

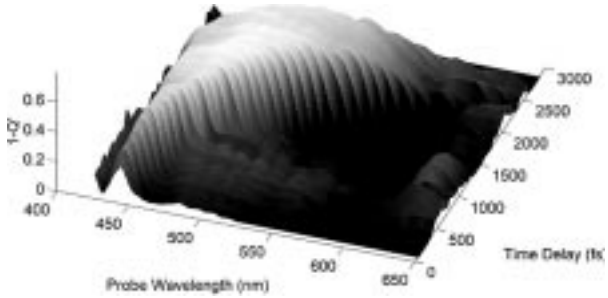

Fig. 7. Continuum probe spectrum (raw data) versus pump-probe delay time as obtained from the spectral measurement of nonlinear absorption for ZnS. Here, $Q' = Q/T_L$ or the nonlinear transmittance Q [(14)] divided by the linear transmittance T_L.

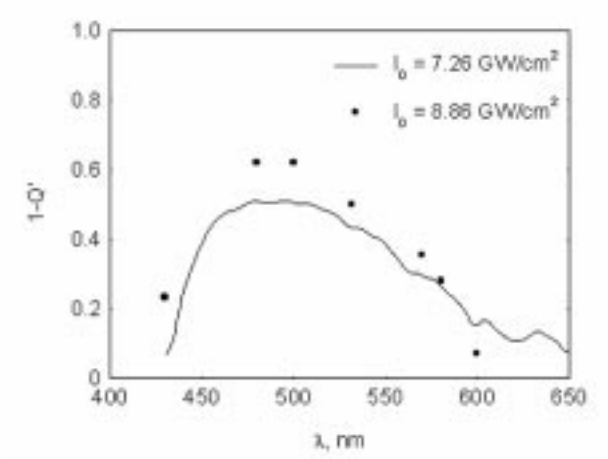

Fig. 8. Differential change in normalized transmittance ($Q' = Q/T_L$) of the WLC pulse versus probe wavelength for ZnS. The solid line is the chirp-corrected envelope of WLC spectra versus time delay (spectral measurement). The solid circles represent the magnitude of the nonlinear transmittance at selected narrowband wavelengths (narrowband measurement).

Fig. 7 contains $Q' = Q/T_L$ [(14)], which is simply the nonlinear transmittance normalized by the linear transmittance. The actual axis is $1 - Q'$ to make the absorption positive and easier to read. The results obtained for ZnS are presented in Fig. 8 for a pump irradiance (inside the sample) of $I_0 = 7.3 \pm 1.5$ GW/cm^2 when the WLC spectrum is recorded. We note that the irradiance calculations have taken into account the small linear absorption of the sample, as well as the Fresnel surface reflections. Furthermore, the WLC beam is focused to a spot size $\sim$5 times smaller than that of the pump beam and therefore we assume the irradiance of the pump is constant over that of the probe beam. For the narrowband measurements, we were limited to seven center wavelengths. These data, for an irradiance of $I_0 = 8.9 \pm 1.8$ GW/cm^2 and the same experimental parameters as for the spectral measurements ($\lambda_P = 0.75$ μm, $w_P = 72$ fs), are also plotted on Fig. 8.

The analytical solution (14) applies to a *bandwidth-limited probe*, i.e., $\sim$5 nm for a bandwidth-limited pulse with $\tau_{\text{wlc}} = 105$ fs in the visible region. In order to fit the experimental data from the WLC spectrum, we have to look at the cross-correlation signal, i.e., the nonlinear absorption versus pump-*bandwidth-limited probe* delay time centered at one particular wavelength in the continuum spectrum. We average the signal over 5 nm ($\sim$5 adjacent pixels on our dual diode array). The only fitting parameter [for ZnS ρ is calculated from (6) and (18)] is the nonlinearity Γ that relates to the 2PA coefficient through (8). The narrow-bandwidth results are detailed in Table I. The best-fitting parameter Γ is listed in the table along with the walk-off values, ρ, at each wavelength.

TABLE I
MATERIAL (ρ) AND NONLINEARITY (Γ) FITTING PARAMETERS FOR NARROWBAND EXPERIMENTS IN ZnS CENTERED AT WAVELENGTH λ

λ, nm	430	480	500	532	570	580	600	620
ρ	27.0	16.4	13.5	9.9	6.9	6.2	5.1	4.1
Γ	4.3	4.5	3.6	1.92	0.85	0.56	0.18	0.08

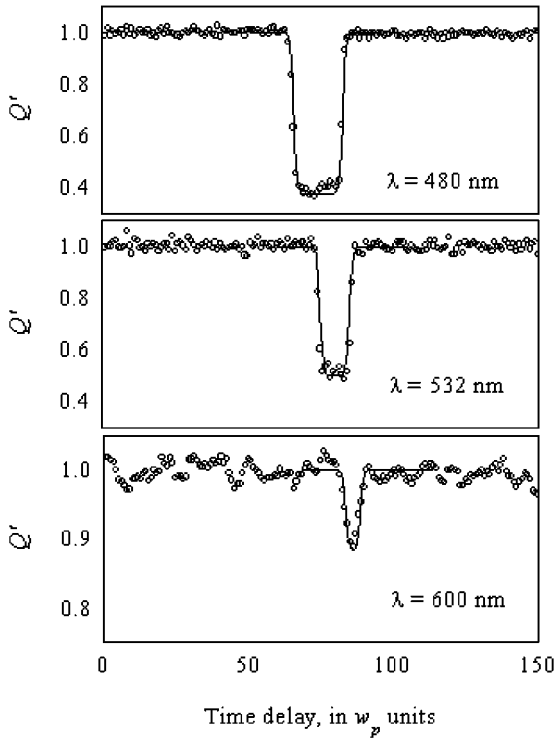

Fig. 9. Normalized *bandwidth-limited probe* fluence transmittance $Q' = Q/T_L$ at λ =480, 532, and 600 nm for ZnS. The solid curves are obtained from fitting the experimental data with (14) and the parameters given in Table I.

For illustration of the fitting procedure, Fig. 9 shows the experimental data (narrowband measurements) and the best curve fit for three central wavelengths: 480, 532, and 600 nm. The value of Q' is plotted versus initial time delay between the pump and *bandwidth-limited probe* pulses. This curve (solid line in Fig. 9) is then translated along the x axis in order to fit the experimental data, since the absolute time is irrelevant here (we work in a coordinate system that moves with the group velocity of the pump pulse). Similar to this analysis, we also fit the cross-correlation signals at several different wavelengths measured with the broadband WLC, i.e., spectral measurement (solid line in Fig. 8).

All the results on the 2PA coefficient β, in cm/GW, for ZnS are shown for comparison in Fig. 10. The solid line (a) is the simplest calculation [(15)], equivalent to the analytical solution in the degenerate case, which completely ignores the temporal walk-off between pump and *bandwidth-limited probe* pulses, i.e., this "data" is not corrected for the effects of temporal walk-

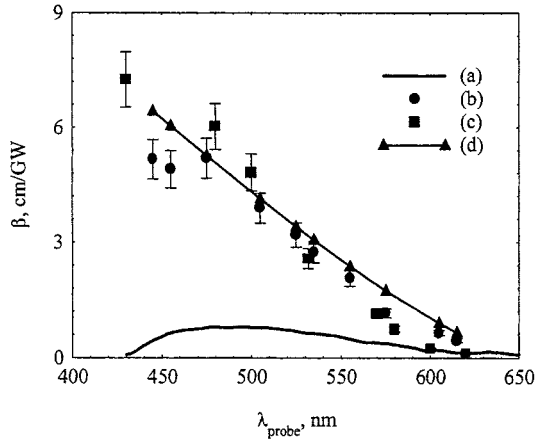

Fig. 10. Nondegenerate two-photon absorption coefficient of ZnS, β, versus *bandwidth-limited probe* wavelength. (a) Spectral measurement, pump-*bandwidth-limited probe* walk-off not included, (15). (b) Spectral measurement with walk-off correction, (14). (c) Narrowband measurement with walk-off correction, (14). (d) Theoretical model for ZnS, $E_g = 3.54$ eV [21]. Parameters used for fitting: $L = 0.84$ mm, $w_p = 72$ fs, $W = 0.85, \lambda_p = 0.75$ μm.

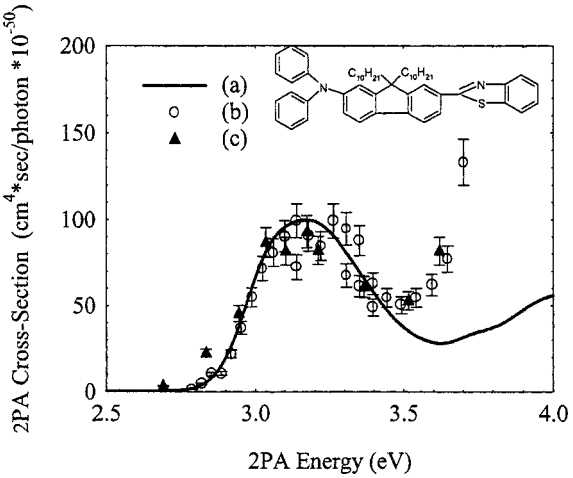

Fig. 11. 2PA of alkyl-fluorene derivative in tetrahydrofuran versus total photon energy: (a) linear absorption spectrum; (b) 2PF data; and (c) white-light continuum pump-*bandwidth-limited probe* measurements with walk-off correction. The fitting parameters are given in Table II. The concentration of the solution is 0.0244 M, and the pathlength is 1 mm.

off. If the complete treatment [results of (14)] is applied to the spectral and narrowband experimental data (Fig. 8), we obtain the filled circles (b) and squares (c) as data points, respectively. Finally, the theoretical predictions for β in ZnS [21] are shown in curve (d). The error bars are due to possible errors in estimating the irradiance of the pump.

The correction provided by the temporal walk-off analysis is appreciable, especially in the short-wavelength range of the WLC probe where the difference between the relative group velocities of the pump and *bandwidth-limited probe* is largest and the effective interaction length is reduced the most. The corrected data not only differ in the magnitude of the 2PA coefficient β, but also dramatically alter the shape of the spectrum. We also note that we achieve good agreement with the predictions of β from the theoretical analysis described in [18]. Furthermore, the close agreement between the spectral method and the narrowband method shows that treating the WLC as a sum of nearly bandwidth-limited pulses centered at different wavelengths is valid. This will be detailed in the Section VI.

V. Comparison to Two-Photon Fluorescence (2PF)

A different method for measuring 2PA spectra that works quite well for fluorescing samples is 2PF spectroscopy [29]. Here, a strong tunable pump beam excites a material via 2PA and the total integrated fluorescence is monitored as a function of input frequency and irradiance. After correcting for the irradiance changes with frequency, and with the assumption that the up-converted fluorescence spectrum is independent of pump frequency (not always the case [30]), the *degenerate* 2PA spectrum is deduced. This method is directly applicable to the burgeoning field of two-photon "confocal" microscopy that can give 3-D images of microscopic samples [3]. A caution in nonlinear spectroscopy is that it can often be difficult to distinguish nonlinear mechanisms. In particular for this discussion is the problem of differentiating excited-state absorption and 2PA. For example, in degenerate 2PA measurements, excited-state absorption can lead to upconversion fluorescence through sequential absorption of two photons. A dependence of the degenerate 2PA cross sections on pump pulsewidth has been observed in early 2PF experiments [29]. The intrinsic 2PA parameters are now measured using picosecond and femtosecond pulses, as opposed to nanosecond experiments that could lead to excited-state absorption enhanced values (as large as 40 times).

The WLC spectrometer presented in this paper gives an alternative method to obtaining NLA spectra of matter. Specifically, the data obtained on organic materials supplements the present knowledge mainly derived from 2PF spectroscopy, with the nondegenerate 2PA spectrum. Two of the benefits of this alternative method are that nonfluorescing samples can also be studied, and given the temporal information obtained from any pump-*bandwidth-limited probe* experiment, it can immediately distinguish between "instantaneous" and long-lived nonlinear processes. We chose an alkyl-fluorene derivative that exhibits excellent green fluorescence to compare the 2PA and 2PF spectroscopy methods. The derivative is a cyclical π-conjugation system with a fluorene backbone and donor-acceptor end groups, and its structure is shown in Fig. 11. The concentration of the solution is 0.024 M, is dissolved in tetrahydrofuran, and the sample pathlength is 1 mm.

The fluorescence measurement is a relative one, and in this case, the results for our sample are calibrated against a well-known reference standard, e.g., fluorescein (the collection geometry inside the fluorimeter apparatus is kept constant for all samples) [31]. The pump wavelength for the nondegenerate measurement is 1.2 μm. The analysis of 2PA raw data follows precisely the procedure outlined for ZnS. The group index measurements performed in this sample were previously shown in Fig. 6 (open triangles). The experimental parameters are as follows: $L = 1$ mm, $w_p = 60$ fs, $W = 1.05, \lambda_p = 1.2$ μm and $I_p^0 = 72.5 \pm 15$ GW/cm^2. With the results for the group indices from the OKE measurements as a starting point, the temporal walk-off parameter, ρ, and the nonlinearity, Γ, are used to fit the experimental cross-correlation signals at fixed *bandwidth-limited probe* wavelengths using the analytical formula (14). The best fitting parameters for several wavelengths

TABLE II
MATERIAL (ρ) AND NONLINEARITY (Γ) FITTING PARAMETERS FOR NARROWBAND EXPERIMENTS IN ALKYL-FLUORENE DERIVATIVE (TETRAHYDROFURAN) CENTERED AT WAVELENGTH λ

λ, nm	480	500	532	570	580	600	620	650	690	750
ρ	3.5	3.2	2.9	2.7	2.65	2.5	2.3	1.9	1.8	1.5
Γ	0.3	0.20	0.24	0.34	0.39	0.35	0.38	0.2	0.1	0.02

are shown in Table II. Fig. 11 shows both the spectrum from the 2PF method along with the WLC spectrum versus the equivalent one-photon absorption energy (i.e., the sum of the energies of the two absorbed photons). The linear absorption spectrum of the solution is also shown (scaled to match in amplitude). For this molecule, which possesses a permanent dipole moment, both single and 2PA are allowed transitions resulting in a similar shape for the linear and nonlinear spectra [32]. We note the two independent measurements of 2PA yield nearly identical nonlinear spectra.

VI. CONCLUSION

We present a method for rapid spectral characterization of two-photon absorbing materials. This should allow the user to substantially increase the database development rate. Knowledge of nonlinear absorption spectra is crucial not only for the development of new devices, but also to determine structure-property relationships for newly developed materials. Furthermore, since this method determines the nondegenerate 2PA spectra, in certain instances, one can infer the dispersion of the nonlinear refractive index which can, in addition to 2PA, be useful in applications including all-optical switching and optical limiting.

A theoretical treatment of the 2PA process in a nondegenerate pump-*bandwidth-limited probe* geometry has been given. The formalism developed takes into consideration temporal pump-*bandwidth-limited probe* walk-off effects. The correction prescribed by this approach is especially significant over spectral regions with large dispersion of the refractive index of the material under study causing the pump and *bandwidth-limited probe* to walk-off each other temporally within the sample, thus reducing the effective interaction length. Hence, the magnitude of the nonlinear signal observed in the experiment is artificially reduced due to poor overlap of the pulses which would lead to inaccurate calculations of the magnitude of the nonlinearity.

We verified the experiment and analysis on the semiconductor ZnS. The good agreement between experimental data and theory for this well-characterized sample (where dispersion effects are large) gives us confidence that the theoretical model for 2PA described in Section II can be applied successfully to other samples, i.e., two-photon absorbing organic dyes that are of great interest for practical applications. As an example, we chose an alkyl-fluorene derivative and used another nonlinear spectroscopy technique, two-photon induced fluorescence, to measure its 2PA spectrum. A comparison of these data with the results obtained from our rapid spectroscopy method shows nearly identical spectra. Note that this is a comparison of the degenerate NLA spectrum with the nondegenerate version. While the theory for this comparison has been developed for semiconductors, this is not the case for organic materials.

We would like to address, in some detail, a few of the assertions made in the sections above. The agreement of our data on ZnS with theory and with previous measurements on this well-characterized sample, verifies that we can make the "dispersionless" approximation as described above and, furthermore, that our neglect of xpm effects between pump and *bandwidth-limited probe* is also valid. We discuss these approximations separately—first dispersion.

The dispersionless approximation we make is essentially the "external self action" limit of Kaplan [33] as applied to the temporal domain. In the external self action limit, which is usually applied to the spatial beam propagation, the beam is assumed to not change its spatial irradiance distribution in propagation through the sample either due to linear diffraction or nonlinear refraction. Here, in the time domain, the dispersionless approximation implies that the pulse temporal distribution does not change with propagation through the thickness of the sample either from linear dispersion or from nonlinear phase modulation. While the full WLC clearly undergoes significant temporal broadening, any nearly bandwidth-limited portion, i.e., the *bandwidth-limited probe*, does not. The broadening of the entire WLC pulse can be described as the individual pulses, which make up the continuum, traveling with different group velocities and therefore separating in time with propagation.

In our experiments, the effects of xpm between the pump and the *bandwidth-limited probe* were minimal. We could determine their magnitude in the organic samples by looking at the shape of the pump-*bandwidth-limited probe* temporal delay curves, as well as by performing the experiments on the neat solvent. The shape of the xpm signals in these continuum experiments, as shown in [24], shows peaks when the pulses overlap near the two sample surfaces (where the two pulses have optimum overlap) along with another oscillation (or oscillations depending on sample thickness) for overlap near the middle of the sample. As Ekvall, *et al.* [24] mention, the xpm signal becomes small for temporal delays where the pulses overlap near the middle of the sample for thick samples. Such effects are specifically due to the large GVM between the two pulses, which is precisely the case in our experiments where the pump wavelength, chosen to be below half the bandgap energy of the sample under study, has a large GVM with respect to the *bandwidth-limited probe* pulses. The 2PA signal in this region remains constant as a function of temporal delay for thick samples or for pump and *bandwidth-limited probe* with large GVM (see Fig. 9, upper curve). Thus, for temporal delays such that the pulses overlap near the middle of the sample, the 2PA signal remains while the xpm signal is small. We, therefore, recommend using thick samples to increase the size of the 2PA signal, provided the dispersionless approximation is still valid. This conclusion is opposite to that made in [24], where they recommend using "dye jets" to have the shortest possible interaction length.

We also note that the key to allowing rapid characterization of these materials is the use of the WLC probe. The assumption that the WLC can be approximated as a sum of independent, *bandwidth-limited probe* pulses is essential in the analysis. The *bandwidth-limited probe* can be considered bandwidth limited if the dispersionless approximation is satisfied. Cross-phase modulation between separate independent *bandwidth-limited probe* pulses can be ignored since they are too weak. However, two

probe pulses can interact through separate xpm interactions with the pump, i.e., the spectra of one gets shifted temporarily into the spectrum of the other. The fact that data taken with a spectrally filtered continuum (narrowband measurements) and the entire WLC (spectral measurements) give the same results shows that these effects can also be ignored, and that it is valid to describe the WLC as a superposition of independent *bandwidth-limited probe* pulses.

The good agreement of our results with past theory and experiments as well as with other spectroscopy techniques gives us confidence that we can utilize this rapid characterization technique to accelerate the study of structure-property relationships in two-photon absorbing organic compounds. We are currently pursuing a study of alkyl-fluorene derivatives similar to the one analyzed in this study. Furthermore, we are comparing our results with other well established degenerate spectroscopy techniques, such as Z-scan. Finally, we are automating both the experimental procedure as well as the data analysis process to truly enhance the speed at which characterization can be achieved.

REFERENCES

[1] S. Kershaw, *Characterization Techniques and Tabulations for Organic Nonlinear Optical Materials*. New York: Marcel Dekker, 1998.

[2] L. W. Tutt and T. F. Boggess, "A review of optical limiting mechanisms and devices using organics, fullerenes, semiconductors and other materials," *Prog. Quantum Electron.*, vol. 17, pp. 299–338, 1993.

[3] W. Denk, J. H. Strickler, and W. W. Webb, "2-photon laser scanning fluorescence microscopy," *Science*, vol. 248, pp. 73–76, 1990.

[4] E. A. Wachter, W. P. Partridge, W. G. Fisher, H. C. Dees, and M. G. Petersen, "Simultaneous two-photon activation of type-I photodynamic therapy agents," in *Proc. SPIE*, vol. 3269, 1998, pp. 68–75.

[5] K. D. Belfield, X. Ren, D. J. Hagan, E. W. Van Stryland, V. Dubikovsky, and E. J. Miesak, "Microfabrication via two-photon photoinitiated polymerization," *Abstr. Papers Amer. Chem. Soc.*, vol. 218, 2001.

[6] M. Sheik-Bahae, A. A. Said, and E. W. Van Stryland, "High sensitivity single beam n_2 measurement," *Opt. Lett.*, vol. 14, pp. 955–957, 1989.

[7] R. R. Alfano, *The Supercontinuum Laser Source*. New York: Springer-Verlag, 1989.

[8] R. L. Fork, C. V. Shank, C. Hirlimann, R. Yen, and W. J. Tomlinson, "Femtosecond white-light continuum pulses," *Opt. Lett.*, vol. 8, pp. 1–3, 1983.

[9] A. Brodeur, F. A. Ilkov, and S. L. Chin, "Beam filamentation and the white light continuum divergence," *Opt. Commun.*, vol. 129, pp. 193–198, 1996.

[10] N. P. Ernsting and M. Kaschke, "A reliable pump-probe, broadband spectrometer for subpicosecond transient absorption," *Rev. Sci. Instrum.*, vol. 62, pp. 600–608, 1991.

[11] E. Tokunaga, A. Terasaki, and T. Kobayashi, "Femtosecond phase spectroscopy by use of frequency-domain interference," *J. Opt. Soc. Amer. B*, vol. 12, pp. 753–771, 1995.

[12] D. C. Hutchings, M. Sheik-Bahae, D. J. Hagan, and E. W. Van Stryland, "Kramers-Krönig relations in nonlinear optics," *Opt. Quantum Electron.*, vol. 24, pp. 1–30, 1992.

[13] V. I. Klimov and D. W. McBranch, "Femtosecond high-sensitivity, chirp-free transient absorption spectroscopy using kHz lasers," *Opt. Lett.*, vol. 23, pp. 1-277–1-279, 1998.

[14] S. Yamaguchi and H. Hamaguchi, "Convenient method of measuring the chirp structure of femtosecond white-light continuum pulses," *Appl. Spectroscopy*, vol. 49, pp. 1513–1515, 1995.

[15] M. Ziolek, M. Lorenc, and R. Naskrecki, "Determination of the temporal response function in femtosecond pump-probe systems," *Appl. Phys. B*, vol. 72, pp. 843–847, 2001.

[16] R. A. Negres, J. M. Hales, A. Kobyakov, D. J. Hagan, and E. W. Van Stryland, "Two-photon spectroscopy and analysis using a white-light continuum probe," *Opt. Lett.*, vol. 27, pp. 270–272, 2002.

[17] P. N. Butcher and D. Cotter, *The Elements of Nonlinear Optics*. Cambridge, U.K.: Cambridge Univ. Press, 1990.

[18] G. P. Agrawal, *Nonlinear Fiber Optics*, 2nd ed. New York: Academic Press, 1995, pp. 50–54.

[19] M. Bass, *Handbook of Optics*, 2nd ed. New York: McGraw-Hill, 1995.

[20] J. A. Bolger, A. K. Kar, B. S. Wherrett, R. DeSalvo, D. C. Hutchings, and D. J. Hagan, "Nondegenerate two-photon absorption spectra of ZnSe, ZnS, and ZnO," *Opt. Commun.*, vol. 97, pp. 203–209, 1993.

[21] E. W. Van Stryland, M. A. Woodall, H. Vanherzeele, and M. J. Soileau, "Energy band-gap dependence of two-photon absorption," *Opt. Lett.*, vol. 10, pp. 490–492, 1985.

[22] P. S. Spencer and K. A. Shore, "Pump-probe propagation in a passive Kerr nonlinear optical medium," *J. Opt. Soc. Amer. B*, vol. 12, pp. 67–71, 1995.

[23] M. Lorenc, M. Ziolek, R. Naskrecki, J. Karolczak, J. Kubicki, and A. Maciejewski, "Artifacts in femtosecond transient absorption spectroscopy," *Appl. Phys. B*, vol. 74, pp. 19–27, 2002.

[24] K. Ekvall, P. van der Meulen, C. Dhollande, L. E. Berg, S. Pommeret, R. Naskrecki, and J. C. Mialocq, "Cross phase modulation artifact in liquid phase transient absorption spectroscopy," *J. Appl. Phys.*, vol. 87, pp. 2340–2352, 2000.

[25] R. A. Negres, "Ultrafast Nonlinear Spectrometer for Materials Characterization," Ph.D. dissertation, Univ. Central Florida, Orlando, 2001.

[26] R. Trebino and D. J. Kane, "Using phase retrieval to measure the intensity and phase of ultrashort pulses: Frequency resolved optical gating," *J. Opt. Soc. Amer. B*, vol. 10, pp. 1101–1111, 1993.

[27] M. Sheik-Bahae, D. C. Hutchings, D. J. Hagan, and E. W. Van Stryland, "Dispersion of bound electronic nonlinear refraction in solids," *IEEE J. Quantum Electron.*, vol. 27, pp. 1296–1309, June 1991.

[28] R. DeSalvo, A. A. Said, D. J. Hagan, E. W. Van Stryland, and M. Sheik-Bahae, "Infrared to ultraviolet measurements of two-photon absorption and n_2 in wide bandgap solids," *IEEE J. Quantum Electron.*, vol. 32, pp. 1324–1333, Aug. 1996.

[29] C. Xu and W. W. Webb, "Measurement of two-photon excitation cross sections of molecular fluorophores with data from 690 to 1050 nm," *J. Opt. Soc. Amer. B*, vol. 13, pp. 481–491, 1996.

[30] K. D. Belfield, S. Andrasik, K. J. Schafer, O. Yavuz, J. M. Hales, and E. W. Van Stryland, "Maleic anhydride-modified polymers for two-photon upconverted fluorescence," *Abstr. Papers Amer. Chem. Soc.*, vol. 221, 2001.

[31] M. Rumi, J. Ehrlich, and A. Heikel *et al.*, "Structure-property relationships for two-photon absorbing chromophores: Bis-donor diphenylpolyene and bis(styryl)benzene derivatives," *J. Amer. Chem. Soc.*, vol. 39, pp. 9500–9510, 2000.

[32] A. F. Garito *et al.*, *Organic Materials for Nonlinear Optics III*. London, U.K.: Royal Soc. of Chemistry, 1989, pp. 16–29.

[33] A. E. Kaplan, "External self-focusing of light by a nonlinear layer," *Radiophys. Quantum Electron.*, vol. 12, pp. 692–696, 1969.

Raluca A. Negres graduated from the University of Bucharest, Bucharest, Romania, in 1993. She received the M.S. and Ph.D. degrees in optical physics from University of Central Florida, Orlando, in 1998 and 2001, respectively. Her dissertation was devoted to ultrafast spectroscopy studies of conjugated organic materials, specifically two-photon and excited-state absorption nonlinear optical processes.

She is currently a post-doctoral Researcher with the Center for Polymers and Organic Solids, University of California at Santa Barbara. Her research focuses on organic light-emitting diodes and semiconducting polymer blends.

Joel M. Hales (M'02) received the B.S. degree from Georgia Institute of Technology, Atlanta, in 1998, and the M.S. degree in optics from the School of Optics/CREOL, University of Central Florida, Orlando, in 2000, where he is currently pursuing the Ph.D. degree in optics.

He was with the Nonlinear Dynamics and Lasers Laboratory, Georgia Institute of Technology, working on low-frequency fluctuations in semiconductor diode lasers. He is currently working on characterizing the chemical structure-nonlinear optical property relationships of organic fluorene derivatives.

Mr. Hales is a member of SPIE and the Optical Society of America.

Andrey Kobyakov (M'01) received the M.Sc. degree (with distinction) in electrical and computer engineering from Moscow Institute of Physics and Technology, Moscow, Russia, in 1992, and the Ph.D. degree in optics (*magna cum laude*) from Friedrich–Schiller University, Jena, Germany, in 1998.

He is currently a Senior Research Scientist at the Photonics Research and Test Center, Corning Incorporated, Somerset, NJ. From 1999 to 2001, he was a Visiting Research Scientist at the School of Optics/CREOL, University of Central Florida, Orlando, where his research involved nonlinear optics with particular emphasis on optical limiting and two-photon absorption spectroscopy. From 1998 to 1999, he was a Research Scientist at the Institute of Solid State Physics and Theoretical Optics, Friedrich-Schiller University, Jena, Germany, where he performed research in spatial solitons, nonlinear waveguide arrays, and optical switching. He has published more than 60 journal and conference papers and has coauthored four book chapters. His current research interests include high-bit-rate large-capacity optical transmission systems, Raman amplifiers, and nonlinear phenomena in fiber optics.

Dr. Kobyakov is a member of the Optical Society of America.

David J. Hagan received the Ph.D. degree from Herriot-Watt University, Edinburgh, U.K., in 1985

He then spent two years as a Research Scientist at North Texas State University, Denton, where he performed research on self-protecting optical limiters. He joined the University of Central Florida, Orlando, in 1987, as a Founding Member of the Center for Research and Education in Optics and Lasers (CREOL) faculty. Since 1991, he has run the School of Optics/CREOL Summer Research Experiences for the undergraduates program, and is also currently the Associate Director for Academic Programs for the School of Optics. He has conducted research on optical limiting devices, fundamental mechanisms for nonlinear absorption and refraction in semiconductors and dielectrics, and cascaded second-order nonlinearities for optical switching devices. More recently, he has been studying nonlinear processes in organics.

Eric W. Van Stryland received the Ph.D. degree in physics from the Optical Sciences Center, University of Arizona, Tucson, in 1976 for work on optical coherent transients and photon-counting statistics.

He worked in the areas of femtosecond pulse production, multiphoton absorption in solids, and laser-induced damage at the Center for Laser Studies, University of Southern California at Los Angeles. He joined the Physics Department at the University of North Texas, Denton, in l978, helping to form the Center for Applied Quantum Electronics. In l987, he joined the newly formed Center for Research and Education in Optics and Lasers (CREOL), University of Central Florida, Orlando, where he was Professor of Physics and Electrical and Computer Engineering. Since July 1999, he has been Director of the School of Optics/CREOL. The National Science Foundation has funded him for the past 25 years, and he has been performing research for the Department of Defense (DoD). He has graduated 22 Ph.D. students and published over 100 papers. He helped develop the Z-scan technique with M. Sheik-Bahae, also with whom he also established the methodology for apply Kramers–Kronig realtions to ultrafast nonlinearities. His current research interests are in the characterization of the nonlinear optical properties of materials and their temporal response, and the applications of these nonlinear material properties for sensor protection, switching, beam control, etc. He also served as a Topical Editor for *Optics Letters*

Dr. Van Stryland is a Fellow of the Optical Society of America, a former member of their Board of Directors, a Senior Member of the Laser Instituute of America, and a former Board Member, a Senior Member of IEEE LEOS, and a member of the SPIE and MRS.